Journal of Applied Research and Technology
ISSN: 1665-6423
jart@aleph.cinstrum.unam.mx
Centro de Ciencias Aplicadas y Desarrollo Tecnológico
México

León-Mancilla, B.H.; Araiza-Téllez, M.A.; Flores-Flores, J.O.; Piña-Barba, M.C.
Physico-chemical characterization of collagen scaffolds for tissue engineering
Journal of Applied Research and Technology, vol. 14, núm. 1, 2016, pp. 1-9
Centro de Ciencias Aplicadas y Desarrollo Tecnológico
Distrito Federal, México

Available online at www.sciencedirect.com

Journal of Applied Research and Technology

CCADET CENTRO DE CIENCIAS APLICADAS Y DESARROLLO TECNOLÓGICO

Journal of Applied Research and Technology xxx (2016) xxx–xxx

www.jart.ccadet.unam.mx

Original

Physico-chemical characterization of collagen scaffolds for tissue engineering

B.H. León-Mancilla [a,*], M.A. Araiza-Téllez [b], J.O. Flores-Flores [c], M.C. Piña-Barba [d,*]

[a] *Departamento de Cirugía, Facultad de Medicina, Universidad Nacional Autónoma de México, Circuito Escolar s/n, Ciudad Universitaria, Del, Coyoacán, México D.F. CP. 04510, Mexico*

[b] *Laboratorio de Biomateriales Dentales, Facultad de Odontología, Universidad Nacional Autónoma de México, México D.F., Mexico*

[c] *Centro de Ciencias Aplicadas y Desarrollo Tecnológico, Universidad Nacional Autónoma de México, Mexico*

[d] *Laboratorio de Biomateriales, Instituto de Investigaciones en Materiales, Universidad Nacional Autónoma de México, Mexico*

Received 24 August 2015; accepted 2 September 2015

Abstract

The objective was to research the physical and chemical properties of collagen scaffolds (CS) obtained from bone matrix Nukbone® subject to a demineralization process using hydrochloric acid. The CS samples were characterized by optical and scanning electron microscopy, elemental chemical analysis, X-ray diffraction, spectroscopy Infrared, thermal analysis, differential scanning calorimetry and nitrogen adsorption. The microanalysis were used to set the macro- and microstructures of CS. They showed that the CS retained the morphology of Nukbone® with interconnected pores and their size between 100 and 500 μm, and it is composed of 20% by weight of HA and the rest is collagen type I. By infrared spectroscopy the functional groups of collagen type I (amide A – 3285, B – 2917, I – 1633, II – 1553 and III – 1239 cm^{-1}) were identified. By thermal analysis it was determined that the phenomenon of denaturation of the collagen type I began in the range of 75–85 °C and burned above 200 °C.

Keywords: Tissue engineering; Collagen scaffolds; Bone matrix; Biomaterials

1. Introduction

In the mid-1980s came the so-called tissue engineering, which has continued to evolve as an exciting and multidisciplinary field, aiming to develop biological substitutes to restore, replace or regenerate defective tissues (Chan & Leong, 2008; Lanza, Langer, & Vacanti, 2013) Tissue engineering mainly uses three factors: scaffolds made of biomaterials must meet certain requirements, cells and growth-stimulating signals, which are known as the triad of tissue engineering. The scaffolds are typically made of polymeric biomaterials, must be biocompatibles and biodegradable upon implantation, with a rate matching that of the new matrix production by the developing tissue; they should be absorbable by the human organism and should be porous with interconnected pores of adequate size to allow cell adhesion and cell proliferation, giving the opportunity to subsequent tissues development, and they must also have the ability to bind to surrounding tissues and be clinically manageable (Langer & Vacanti, 1993).

There are a great variety of choices to select scaffolds for tissue engineering; in general, the biomaterials used for making porous scaffolds can be classified into two categories according to their sources, natural and synthetic (Meyer, Meyer, Handschel, & Wiesmann, 2009). The natural biomaterials generally have excellent biocompatibility so that the cells can adhere and grow with excellent viability. In this sense, the scaffolds can be obtained from different animal species: pigs, bovine and horses, using intestine, pericardium, skin, tendon, bone and demineralized bone (Carletti, Motta, & Migliaresi, 2011; Chen, Torian, Price, & McKittrick, 2011).

* Corresponding authors.
E-mail addresses: benleonman@gmail.com (B.H. León-Mancilla), crispina99@gmail.com (M.C. Piña-Barba).

Peer Review under the responsibility of Universidad Nacional Autónoma de México.

http://dx.doi.org/10.1016/j.jart.2016.01.001

Please cite this article in press as: León-Mancilla, B. H., et al. Physico-chemical characterization of collagen scaffolds for tissue engineering. *Journal of Applied Research and Technology* (2016), http://dx.doi.org/10.1016/j.jart.2016.01.001

The main objective of this work was to determine the physicochemical properties of collagen scaffolds (CS), produced by immersion of bone matrix (BM) blocks in hydrochloric acid (HCl) at 0.5 M, through different characterization techniques: the histological studies were made with optical microscopy (OM) using the following stainings: hematoxylin & eosin (H&E) (Montuenga Badía & Calvo Gonzáles, 2009), von Kossa (Penney, Powers, Frank, Willis, & Churukian, 2002), Masson's Trichrome (Sampedro, 2014) and polarized light (Narváez, 2014). Scanning electronic microscopy (SEM) and energy dispersive spectrometry (EDS) (Vázquez & Echeverría, 2000); thermogravimetric analysis (TGA) and differential scanning calorimetry (DSC) (Skoog, Holler, & Crouch, 2008); Fourier transform infrared spectrometry (FTIR) (Coman, Grecu, Baciut, Prodan & Simon, 2007; Griffiths & De Haseth, 2007) the total area was measured using N_2 adsorption (BET) (Nishad, Dhathathreyan & Ramasami, 2002) was measured. For each technique at least 5 samples were used.

The collagen scaffolds characterized in this work were obtained from Nukbone®, bone matrix whose pores are interconnected in a range of size from 100 to 500 μm that allow the cellular growth, and were already used without cells in patients with bone defects, successfully (Aguilar, Piña, López, Rodríguez, & Driessens, 2005; Piña, Munguía, Palma & Lima, 2006; Cueva-Del Castillo et al., 2008; León, Araiza, & Piña, 2012; Rodríguez et al., 2013).

2. Material and methods

2.1. Sample preparation

Blocks of Nukbone® (BM) of 2.5 cm × 2.5 cm × 0.5 cm were employed, and each one was immersed for 10 min in stirring in 50 mL of chloridric acid (HCl) (TJ Baker, Germany) solution with bidistilled water at 0.5 M. Then they were rinsed with bidistilled water and dried, thus collagen scaffolds were obtained, as shown in Figure 1.

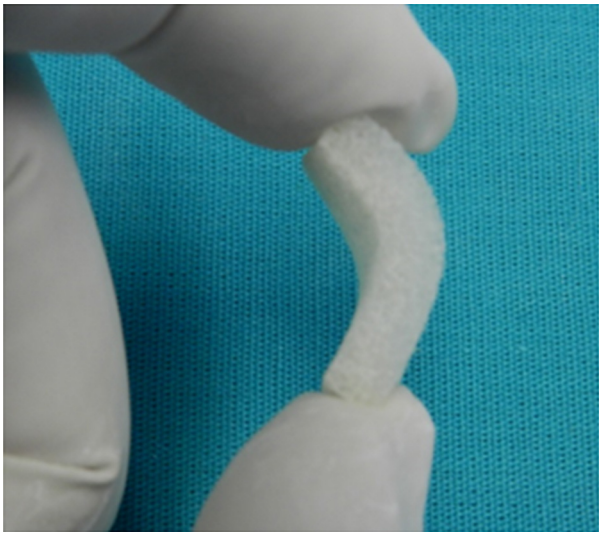

Fig. 1. Collagen scaffolds (CS).

2.2. Optical microscopy (OM)

To perform histological studies collagen scaffolds cubes of 1 cm × 1 cm × 0.5 cm were used; they were dehydrated in alcohols at different concentrations: 50, 60, 70, 80, 96 and 100%, in an histoquinet during 2 h in each concentration and then were included in wax cubes and 3 μm thick slices were cut with a microtome.

To determine the internal structure of the CS, bright-field microscopy was used. The samples of CS were cut into slices of 3 μm thickness. The samples were stained using hematoxylin & eosin (H&E), Masson's Trichrome (MT), von Kossa (vK), and they were also observed using polarized light microscopy (PLM).

2.3. Scanning electron microscopy (SEM) and elemental chemical analysis (EDS)

The microstructure of samples was analyzed with a JEOL electron microscope JSM7600F, using the technique of secondary electrons with a voltage of 5 kV. The size of the samples used in SEM was 1 cm × 1 cm × 0.5 cm, and no sample was covered with conductive material; they were placed directly in the sample holder. EDS technique was also employed for determining the main compounds of different superficial zones.

2.4. X-ray diffraction (XRD)

The powders of BM and CS were tested by an X-ray diffractometer D8 Advance of Bruker AXS, with Cu Kα radiation ($\lambda = 0.154$ nm) and 2θ from 18° to 80°, to obtain structural information on an atomic scale from both materials (BM and CS).

2.5. Fourier transform infrared (FTIR)

To identify the functional groups of collagen used the Fourier transform infrared (FTIR) analysis of CS was done with a Scientific Nicolet™ 6700 FT-IR spectrometer, in a wave number range of 500–3500 cm^{-1}; the samples of 0.2 cm thickness were placed directly in the spectrometer.

2.6. Thermo gravimetric analysis (TGA)–differential scanning calorimetry (DSC)

The behavior of the samples with temperature was studied using TA Instruments SDTQ600 in nitrogen atmosphere. TGA and DSC curves were taken in the range 25–700 °C at a heating rate of 10 °C/min.

2.7. Nitrogen adsorption (BET)

The total area of the samples was determined using a Quantachrome Instruments Autosorb equipment, employing cubes of 20 mm × 20 mm × 20 mm of BM and CS were used. The analysis was carried out using liquid nitrogen, and the samples

Please cite this article in press as: León-Mancilla, B. H., et al. Physico-chemical characterization of collagen scaffolds for tissue engineering. *Journal of Applied Research and Technology* (2016), http://dx.doi.org/10.1016/j.jart.2016.01.001

were cleaned prior to the analysis at 77 K. The area was determined before and after the demineralization process (Chen & McKittrick, 2011)

3. Results and discussion

3.1. Preparation of samples

Actually, HCl is used for demineralization of hard tissue with allograft purposes, as reported by Gruskin, Doll, Futrell, Schmitz, and Hollinger (2012), or for obtaining matrices from demineralized human and bovine bone, for use in tissue engineering; Murugan et al. reported 3 days of treatment to demineralize the samples of 10 mm^3 at environment temperature (Murugan, Ramakrishna, & Rao, 2008); meanwhile our treatment requires only 10 min.

The results showed that the demineralization of bone matrix using HCl did not alter its structure and hold the organic compound that was identified as type I collagen.

3.2. Optical microscopy (OM)

The samples of CS cut into 3 μm thick slices were used in bright-field optical microscopy, with several staining techniques mentioned above.

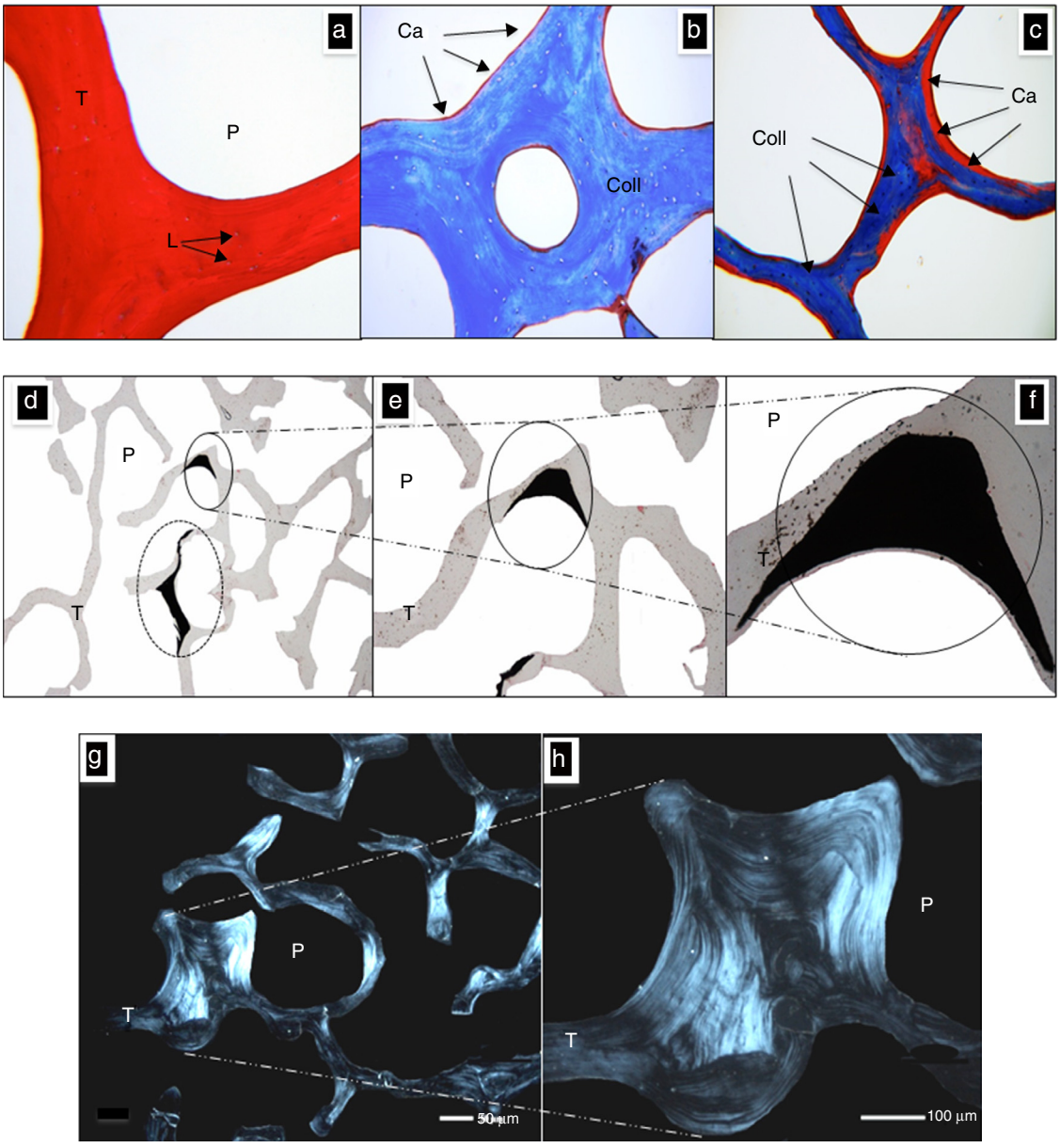

Fig. 2. Morphological characterization with optical microscopy. (a) CS stained with H&E, pores (P) and trabecules (T) with multiples lacunae (L) can be seen. (b) CS stained with Masson's Trichrome, identifying the fiber of collagen (Coll) with a blue color and residue of calcium (Ca) identified by red color. (c) Elsewhere in the CS in which a higher concentration of Ca is observed. a–c: 100×. (d–f) CS stained with von Kossa technique. The dark areas involving a higher concentration of calcium remaining after demineralization. P denotes a pore, T denotes a trabecula and Ca denotes calcium. d: 10×, e: 40×, f: 100×. (g and h) Photographs of the CS taken with polarized light; the collagen fibers orientation gives the architecture of bone trabeculae (T) and the pores (P). g: 10×, h: 40×.

Please cite this article in press as: León-Mancilla, B. H., et al. Physico-chemical characterization of collagen scaffolds for tissue engineering. *Journal of Applied Research and Technology* (2016), http://dx.doi.org/10.1016/j.jart.2016.01.001

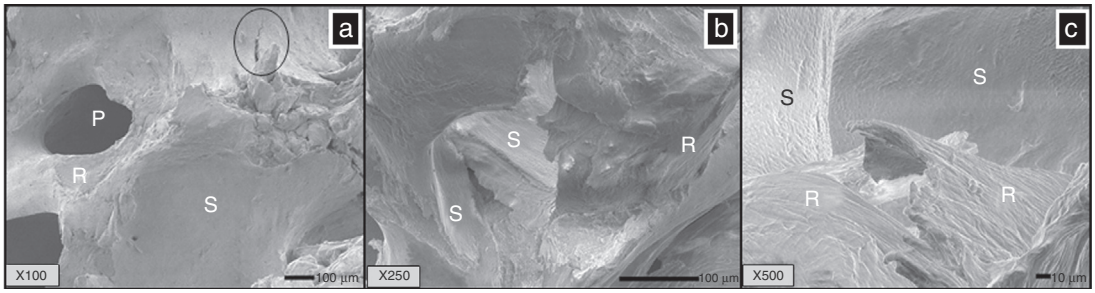

Fig. 3. (a) Bone matrix (BM) observed by SEM, pores are observed (P) and a smooth zone corresponding to the surface of HA (S), and a rough area (R) lacking of HA, corresponding to collagen fibers. SEM images of CS (b and c) showed two areas well identified; the smooth (S) surface corresponded with the area of HA which was removed by the demineralization process. The other zone was observed as rough (R) corresponding to collagen fibers. a: 100×, b: 250×, c: 500×.

Figure 2a shows a cut of CS stained with H&E; **P** denotes the space of a pore while **T** denotes the space occupied by a trabecula, now without the ceramic component. The morphology of this tissue is observed with eosinophilic pigment (red), thus expressing its affinity by the organic structure, which in this case is the collagen. The bone gaps were spaces (**L**) occupied by osteocytes, preserved their architecture (size and form), and they were basophilic pigmented (blue), which matches with description reported by Domínguez and Torres (2006).

Meanwhile Figure 2b and c shows a 3 μm thickness histological section of CS stained with Masson's technique where the structure was occupied by a trabecula meshwork, now without ceramic compound. Here, the red color denotes the calcium presence (Ca) and the blue color denotes collagen (Coll); it is possible to see that the calcium is found mostly on the edges, and it is not distributed uniformly in the volume as could be expected.

Von Kossa staining, shown in Figure 2d–f, is employed to determine Ca concentration in new formation tissue (Zong Ming, Jian Yu, Rui Xin, Hao, & Yong, 2013). This stain allows to observe the concentration Ca places; these places are related with the sites where the HA is associated with the collagen in Masson's stain, observed in Figure 2c (in red color). In Figure 2e only two dark zones correspond to high concentration of Ca, and in the rest of the body of CS, small sites of Ca were observed. The architecture of trabeculae is conserved; in Figure 2f the details of the deposition of Ca including a circle way of the trabeculae are shown.

Figure 2g and h are cuts of 3 μm thickness; these images were obtained with a polarized light microscope, and it corresponds to the collagen of a trabeculae. This technique showed how the collagen fibers are arranged in bundles that determine the final morphology of the bone matrix and the scaffolds; the pores are preserved and their sizes varied in the range of 100–500 μm.

3.3. Scanning electron microscopy (SEM) and elemental chemical analysis (EDS)

Figure 3a (X100) shows the microstructure of the BM; three zones may be seen; one of them is rough (R) and corresponds to a cut from trabecula; another zone is smooth (S) which corresponds to the extern surface of the trabeculae constituted by hydroxyapatite (ceramic component of the bones), and the last zone is a porous zone (P), that corresponds to opened and interconnected pores, which have a range size of 100–200 μm, and a fracture (circle) due to excessive charge of compression is also observed.

Figure 3b shows a photomicrograph of CS (X250); it is interesting to note two different surfaces; one of them is a smooth zone feature to hydroxyapatite (HA, main compound of bone) and which maintains its morphology (S) and is covering to rough volumes (R) that correspond to the trabecula conformed by collagen fibrous; this fact speaks of the kindness of the demineralization method.

Figure 3c (X500) also shows a microstructure of CS, and it can be seen that the exterior surface (S) retains its smooth morphology while the volume is made of long fibers as expected. This was also reported by Chen & McKittrick, (2011).

3.4. Macropores measured by SEM

Through SEM the pore size before and after demineralization was compared. Figure 4a and b are SEM images (X50), and they allowed measurements to the bone matrix, first mineralized (BM) and after demineralized (CS). The pores were measured and there was no difference in the measurements before and after demineralization. The pore sizes remained in a range of 180–350 μm. Murphy reported that the optimum pore size to promote cell proliferation and migration in bone tissue engineering is 325 microns (Murphy, Haugh, & O'Brien, 2010). The pores generally have an oval shape that the largest diameter was in a range between 100 and 500 μm, and was ideal for use as a cell scaffold.

3.5. Energy dispersive X-ray analysis (EDS)

Elemental analysis was made using EDS of the smooth and rought areas identified by SEM in Figure 4a and b, to be punctual is a semiquantitative analysis. On the surface, the identified elements of higher percentage in weight were: O (41.34%); Ca (29.36%); C (16.08%); P (12.16%); Mg (0.66%) and Na (0.39%) that can be associated to calcium phosphates like HA, as observed in Figure 3a. In the fibrous zone under the surface, the identified elements were C (43.92%), N (23.87%) and O (23.87%); these elements are part of the amide functional groups of the collagen (NH, C=O) between others, as observed in Figure 3c. In Table 1, the elements found on CS and their proportion are reported.

Please cite this article in press as: León-Mancilla, B. H., et al. Physico-chemical characterization of collagen scaffolds for tissue engineering. *Journal of Applied Research and Technology* (2016), http://dx.doi.org/10.1016/j.jart.2016.01.001

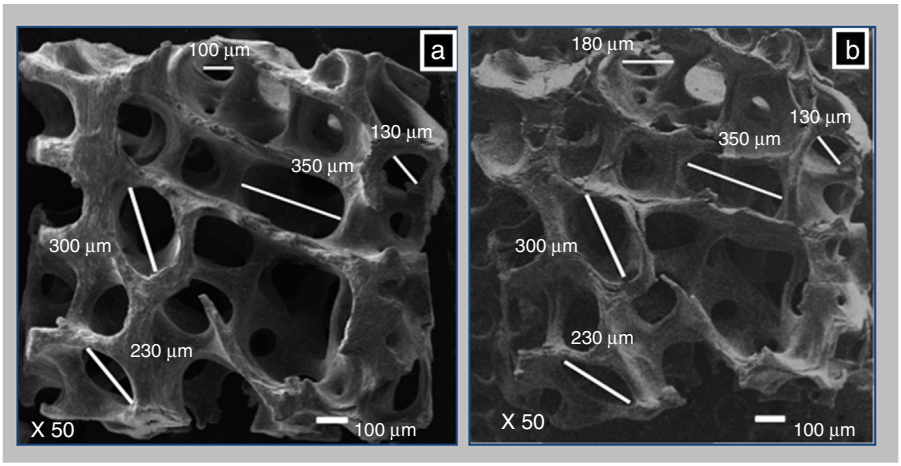

Fig. 4. SEM images showing the effect of demineralization process in the morphology and structure of BM (a). There were no significant changes as a result of demineralization in distribution of pores, neither in shape nor size, thus preserving the three dimensional structure in the CS (b).

Table 1
Elemental analysis by EDS of collagen scaffolds.

Element	Inorganic area Weight %	Organic area Weight %
C	16.08	43.92
O	41.34	31.41
P	12.16	–
Na	0.39	–
Mg	0.66	–
Ca	20.36	–
N	–	23.87

3.5.1. X-ray diffraction (XRD)

The XRD of BM and CS is shown in Figure 5 and was compared with the data sheet 9-432 from Joint Committee Powder Diffraction (JCDP), of PDF-2 (Powder Diffraction Field) of International Center for Diffraction Data (ICDD, 2006), that corresponds to hydroxyapatite, mineral compound of bone, which is a crystalline ceramic. The diffractogram of the CS appears as an amorphous material; however, the main peaks of HA: $2\theta = 25.8$ (002), $2\theta = 30.4$ (121), $2\theta = 30.6$ (112), $2\theta = 32.9$ (300) are distinguished, which indicates that a certain amount of it is present in the sample.

3.6. Infrared spectroscopy (FTIR)

The results obtained through this technique allow us to identify the functional groups of the organic part of the CS, see Figure 6. However, there is a phosphate group PO_4 (1076 cm^{-1}), corresponding to remainder hydroxyapatite (Xiao, Cai, & Liu, 2007). Functional groups identified in the IR spectra were amide A, B, I, II and III corresponding to collagen (Xiao et al., 2007).

The sample of CS shows the following bands: 1650–1665 cm^{-1} (C=O) corresponding to Amide I; 1530–1550 cm^{-1} corresponding to Amide II $\delta(NH) + \nu(CN)$; 3325–3330 for Amide A (N–H); the peaks at 2956 cm^{-1} corresponding to functional group CH_3; 2924 cm^{-1} to CH_2; 1239 cm^{-1} to Amide III $\delta(NH) + \nu(CN)$; and 3080 cm^{-1} to Amide B (CH_2) can be seen. Those functional groups are corresponding to collagen (Sionkowska & Kozłowska, 2010). Table 2 summarizes the data obtained for the CS IR spectra.

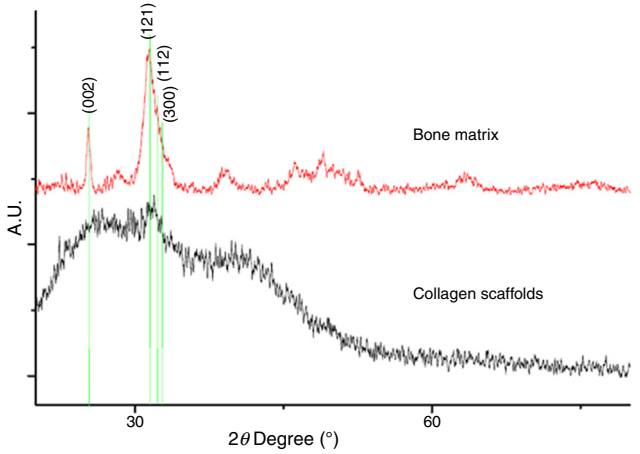

Fig. 5. X-ray diffractograms for bone matrix (BM) and collagen scaffold (CS). The reference peaks correspond to JCPD 9-432 file.

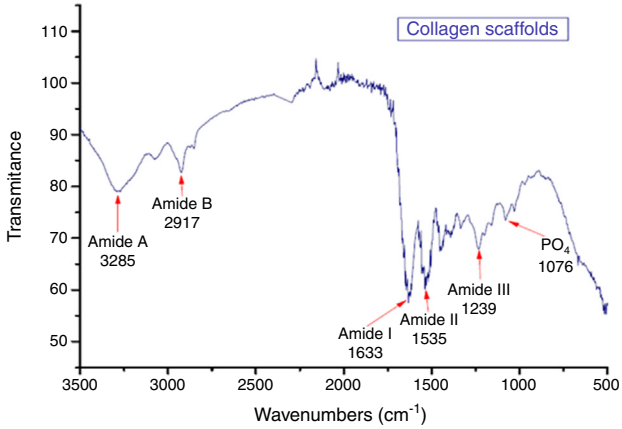

Fig. 6. Infrared spectra of CS where functional groups for amides (A, B, I, II, III) and phosphate (PO_4) are identified.

Please cite this article in press as: León-Mancilla, B. H., et al. Physico-chemical characterization of collagen scaffolds for tissue engineering. *Journal of Applied Research and Technology* (2016), http://dx.doi.org/10.1016/j.jart.2016.01.001

Table 2
Infrared spectrum.

Functional groups	IR (cm^{-1})	IR of CS
CH_3	2956	–
CH_2	2924	–
Amide I (C=O)	1650–1665	1633
Amide II δ(NH) + ν(C-N)	1530–1550	1535
Amide III δ(NH) + ν(C-N)	1239	1239
Amide A (NH)	3325–3330	3285
Amide B (CH_2)	3080	2917

3.7. Thermo gravimetric analysis (TGA)

The TGA provided information about the behavior with the temperature presented by the BM (Fig. 7a) as compared with CS (Fig. 7b). The main loss is presented in three different temperature ranges given by A: (50–200 °C); B: (200–450 °C) and C: (450–700 °C), as shown in Figure 7a and b. The curve in A corresponded to the loss of the physisorbed and chemical water in the material, which represented the 6.07%wt of the bone matrix, which occurred at 79 °C. Meanwhile for CS the loss of water corresponded to 9.6%wt and occurred at 114.74 °C. These findings are similar to those reported by Lozano, Peña & Heredia, (2003).

The following loss, occurring in the range of temperatures B in the thermogram, for BM was observed between 341 and 493 °C corresponding to 30.34 wt% loss compared to 67.76% corresponding to 311.63 °C for CS. These losses are related to the combustion of collagen in the two samples. The differences in mass loss in the BM could be due to the structure

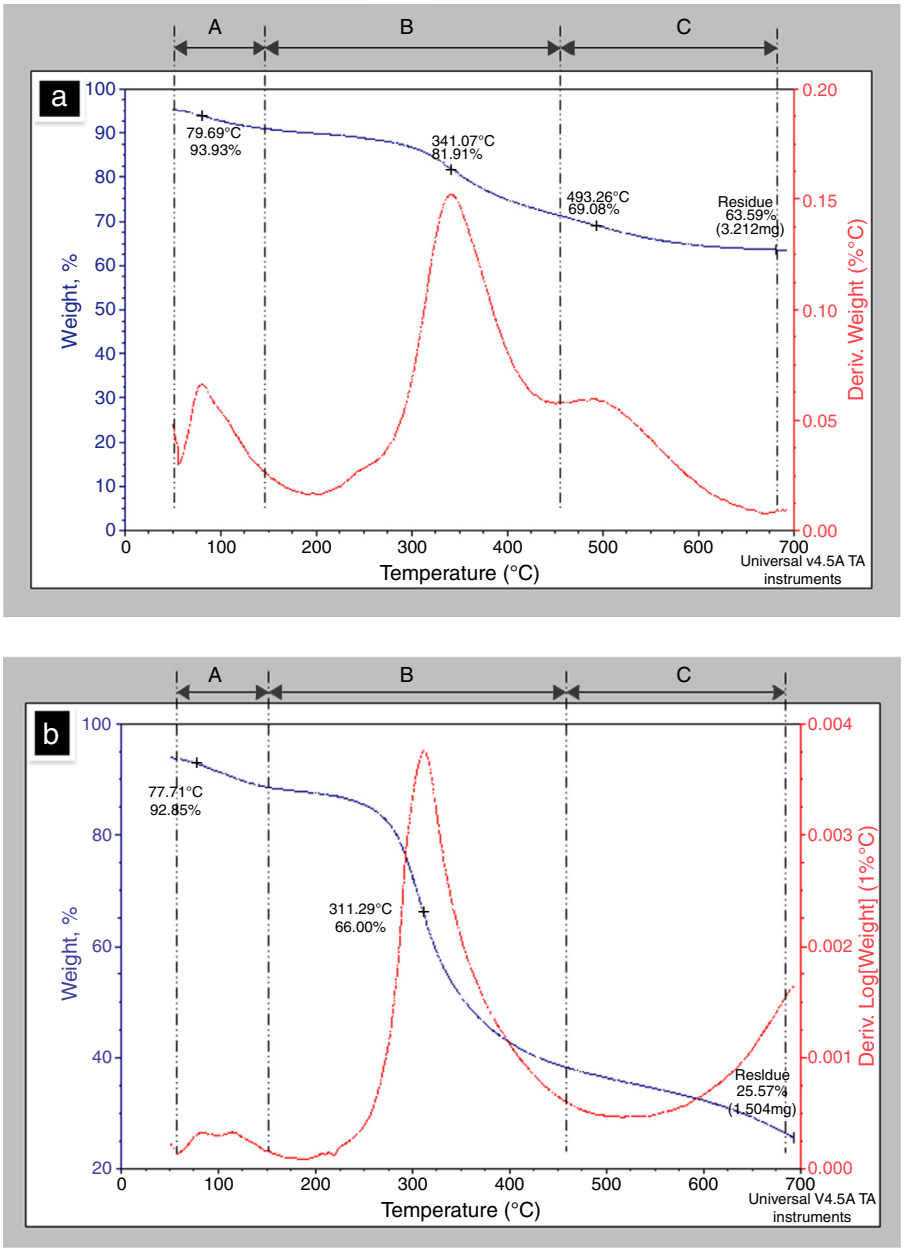

Fig. 7. (a) TGA graph of bone matrix (BM), upper line corresponds to the weight loss and lower line is the derivative curve ($\Delta\omega/\Delta T$). (b) TGA graph of collagen scaffold (CS).

Please cite this article in press as: León-Mancilla, B. H., et al. Physico-chemical characterization of collagen scaffolds for tissue engineering. *Journal of Applied Research and Technology* (2016), http://dx.doi.org/10.1016/j.jart.2016.01.001

Table 3
Thermograms data for bone matrix and collagen scaffold.

Condition	BM		CS	
	Mass loss (%)	°C	Mass loss (%)	°C
Dehydrated collagen denaturalized	6.07	79.69	9.6	114.76
Collagen combustion	30.34	341/493	64.76	311.63
Remainder	63.59	700	25.64	700

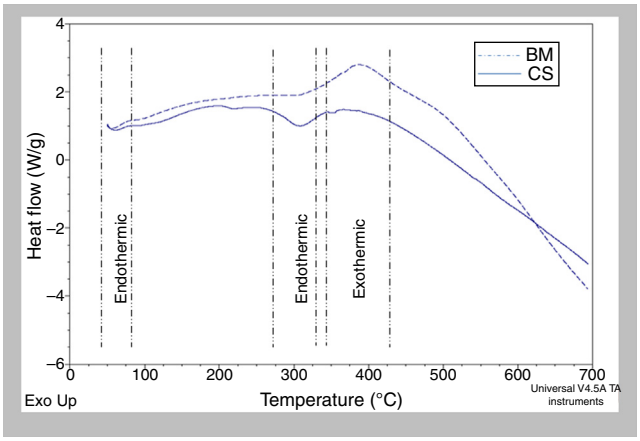

Fig. 8. Comparative DSC analysis of the bone matrix (dotted line) and of scaffold collagen (continuous line).

of the trabeculae devoid from mineral phase (HA), so that the combustion occurs at a lower temperature. Finally, the weight loss in C, corresponding to 450–700 °C, presenting a minimum change in mass loss, leaving a residue of 63.59% for the BM and 25.64% for CS surely corresponds to calcium compounds. The use of derivative of thermal analysis (DTG) allowed determining that the degradation process of collagen had maximum rate at 311.95 °C. The data obtained from the thermograms for BM and CS are summarized in Table 3.

3.8. Differential scanning calorimetry (DSC)

This technique allowed to identify changes in the thermodynamic variables that occurred during the physic-chemical transformations induced by heating or cooling the BM and CS. The first endothermic peak observed in BM and CS was between 85 and 90 °C, corresponding to dehydration process of surface water, see Figure 8. This result is also presented in the study by Lozano et al. (2003). The second endothermic phenomenon observed in the BM and CS was in the temperature range between 275 °C and 325 °C. This is related to the loss of hydrogen bonds, so that the phenomenon of protein denaturation, could be initiated in this interval in which the tertiary structure is lost. This phenomenon is reversible if the protein is newly hydrated.

An exothermic process was found in both samples (BM and CS) observed in a temperature range between 350 °C and 425 °C, corresponding to the combustion of the collagen fibers. The results obtained with the DSC technique are complemented by TGA, which suggests that BM and CS are basically composed of three components, which are water, collagen and hydroxyapatite.

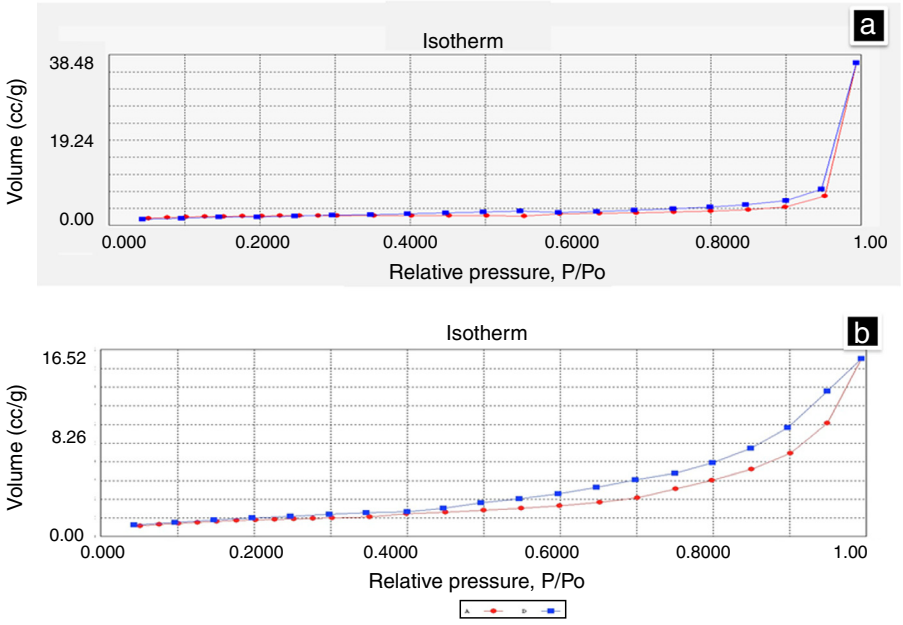

Fig. 9. N_2 physisorption curves recorded at 77 K of bone matrix (a) and collagen scaffold (b). Line red: adsorption, line blue: desorption.

Please cite this article in press as: León-Mancilla, B. H., et al. Physico-chemical characterization of collagen scaffolds for tissue engineering. *Journal of Applied Research and Technology* (2016), http://dx.doi.org/10.1016/j.jart.2016.01.001

Table 4
Total area BET under IUPAC classification.

	Surface area (m^2/g)	Isotherm	Pore size	Pore form
BM	5.39	Type II	Macroporous	Open
CS	7.34	Type II	Macroporous	
Difference	36.18%			

3.9. Nitrogen adsorption (BET)

The total area of the BM was determined by BET and was compared with the area of CS. The results obtained were 5.39 m^2/g for BM and 7.34 m^2/g for CS. The difference of the total surface area between the BM and CS was 36.18%, the result can be used for in vitro studies, because it is the area that will be in contact with the cells. Figure 9a shows the isotherm presented by the BM, and it shows that there were no changes (hysteresis) between adsorption (red line) and desorption (blue line). Figure 9b is the isotherm from CS, and there is a minimum difference between the adsorption and desorption of gas. The isotherms observed are Type 2 and correspond to an open macropores type, according to the IUPAC. Table 4 summarizes all data obtained.

4. Conclusions

These scaffolds have the advantage that they can be molded to give them different shapes. The scaffolds preserved the morphology from trabecular bone, the pores are open and interconnected, and the pore sizes are adequate for use as cell scaffolds (tissue regeneration). This biomaterial is proposed for use as a scaffold in tissue regeneration. The collagen scaffolds obtained are completely biocompatible, biodegradable and easy to use.

Acknowledgments

Thanks to E. Fregoso, V. Rodríguez, A. Pérez, O. Novelo, A. Tejeda, M.A. Canseco, M. Herrera, A. Zepeda, F. Pasos and V. Maturano for their technical support. Also thanks to DGAPA-UNAM for financial support through projects: IG100114, IT114911, IT119111 and IN113108.

References

Aguilar, M., Piña, M. C., López, R., Rodríguez, L., & Driessens, F. (2005). Cytotoxic and genotoxic effects of the exposition of human lymphocytes to a ceramic material in vitro. *Journal Applied Biomatrials Biomechanics*, *3*(1), 29–34.

Carletti, E., Motta, A., & Migliaresi, C. (2011). Scaffolds for tissue engineering and 3D cell culture. *Methods in Molecular Biology*, *695*, 17–39.

Chan, B. P., & Leong, K. W. (2008). Scaffolding in tissue engineering: general approaches and tissue specific considerations. *European Spine Journal*, *17*(Suppl 4), S467–S479.

Chen, P. Y., Torian, D., Price, P. A., & McKittrick, J. (2011). Mineral form a continuum in mature cancellous bone. *Calcification Tissue International*, *88*, 351–361.

Chen, P. Y., & McKittrick, J. (2011). Compressive mechanical properties of demineralized and deproteinized cancellous bone. *Journal of the Mechanical Behavior of Biomedical Materials*, *4*, 961–973.

Coman, V., Grecu, R., Baciut, M., Baciut, G., Prodan, P., & Simon, V. (2007). Investigation of different bone matrices by vibrational spectroscopy. *Journal Optoelectronics Advanced Material*, *9*(11), 3372–3375.

Cueva-Del Castillo, J. F., Valdés-Gutiérrez, G. A., Elizondo-Vázquez, F., Pérez-Ortiz, O., Piña, B. M., & León-Mancilla, B. H. (2008). Bone loss treatment, pseudoarthrosis, arthrodesis and benign tumors using xenoimplant: clinical study. *Cirugía y Cirujanos*, *77*(4), 267–271.

Domínguez, A. A., & Torres, V. K. (2006). Descripción histológica de la regeneración ósea en conejos implantados con hueso de bovino liofilizado (Nukbone). *Investigación Universitaria Multidisciplinaria*, *5*(5), 27–35.

Griffiths, P. R., & De Haseth, J. A. (2007). *Fourier transform infrared spectrometry* (2nd ed.). New Jersey: John Wiley & Sons. ISBN: 978-0-471-19404-0.

Gruskin, E., Doll, B. A., Futrell, F. W., Schmitz, J. P., & Hollinger, J. O. (2012). Demineralized bone matrix in bone repair: History and use. *Advanced Drugs Delivery Reviews*, *64*(12), 1063–1077.

Langer, R., & Vacanti, J. P. (1993). Tissue engineering. *Science*, *260*(5110), 920–926.

Lanza, R., Langer, R., & Vacanti, J. P. (2013). *Principles of tissue engineering* (4th ed.). San Diego: Elsevier Academic Press. ISBN: 978-0-12-398358-9.

León, B. H., Araiza, M. A., & Piña, M. C. (2012). Scaffolds of collagen from Nukbone®. *Materials Research Society Proceedings*, *1487* http://dx.doi.org/10.1557/opli.2012.1528, imrc12-s4b-p039

Lozano, L. F., Pena-Rico, M. A., Heredia, A., Ocotlan-Flores, J., Gomez-Cortes, A., Velazquez, R., et al. (2003). Thermal analysis study of human bone. *Journal of Materials Sciences*, *38*, 4777–4782.

Meyer, U., Meyer, T., Handschel, J., & Wiesmann, H. P. (2009). *Fundamentals of tissue engineering and regenerative medicine*. Berlin: Springer Verlag. ISBN: 978-3-540-77754-7.

Montuenga Badía, L., & Calvo Gonzáles, A. (2009). *Técnicas en Histología y Biología Celular*. Barcelona: Elsevier Masson. ISBN: 978-84-458-1964-7.

Murphy, C. M., Haugh, M. G., & O'Brien, F. J. (2010). The effect of mean pore size on cell attachment, proliferation and migration in collagen glycosaminoglycan scaffolds for bone tissue engineering. *Biomaterials*, *31*, 461–466.

Murugan, R., Ramakrishna, S., & Rao, K. P. (2008). Analysis of bovine derived demineralized bone extracts. *Journal of Materials Sciences: Materials in Medicine*, *19*, 2423–2426.

Narváez, A. D. Microscopía Óptica. http://medic.ula.ve/histologia Accessed January 2014.

Nishad, N., Dhathathreyan, A., & Ramasami, T. (2002). Mercury intrusion porosimetry, nitrogen adsorption, and scanning electron microscopy analysis of pores in skin. *Biomacromolecules*, *3*, 899–904.

Penney, D. P., Powers, J. M., Frank, M., Willis, C., & Churukian, C. (2002). Analysis and testing of biological stains – The Biological Stain Commission Procedures. *Biotechnic and Histochemistry*, *77*, 237–275.

Piña, B. M. C., Munguía, A. N., Palma, C. R., & Lima, E. (2006). Caracterización de hueso de bovino anorgánico: Nukbone. *Acta Ortopédica Mexicana*, *20*(4), 150–155.

Rodríguez, F. N., Rodríguez, H. A. G., Enríquez, J. J., Alcántara, Q. L. E., Fuentes, M. L., Piña, B. M. C., et al. (2013). Nukbone® promotes proliferation and osteoblastic differentiation of mesenchymal stem cells from human amniotic membrane. *Biochemical and Biophysical Research Communications*, *434*(3), 676–680.

Sampedro, C. E. (2014). *Coordinación de Enseñanza, Departamento de Biología Celular y Tisular*. Facultad de Medicina, UNAM. http://wwwfacmed.unam.mx. Accessed January 2014

Sionkowska, A., & Kozłowska, J. (2010). Characterization of collagen/hydroxyapatite composite sponge as a potential bone substitute. *International Journal of Biological Macromolecules*, *47*, 483–487.

Skoog, D. A., Holler, F. J., & Crouch, S. R. (2008). *Principios de Análisis Instrumental* (6a ed.). México D.F.: CENGANE Learning. ISBN: 978-970-686-829-9

Please cite this article in press as: León-Mancilla, B. H., et al. Physico-chemical characterization of collagen scaffolds for tissue engineering. *Journal of Applied Research and Technology* (2016), http://dx.doi.org/10.1016/j.jart.2016.01.001

The International Centre for Diffraction Data (ICDD). 2006. Joint Committee Powder Diffraction (JCPD). Powder Diffraction File (PDF). www.icdd.com Acceded January 2015.

Vázquez, N. G., & Echeverría, O. (2000). *Introducción a la Microscopia Electrónica Aplicada a las Ciencias Biológicas*. México D.F.: Fondo de Cultura Económica. ISBN: 968-16-6240-7

Xiao, H., Cai, G., & Liu, M. (2007). Hydroxyl radical induced structural changes of collagen. *Spectroscopy*, *21*(2), 91–103.

Zong Ming, W., Jian Yu, L., Rui Xin, L., Hao, L., & Yong, G. (2013). Bone formation in rabbit cancellous bone explant culture model is enhance by mechanical load. *Biomedical Engineering Online*, *12*(35), 1–15.

Please cite this article in press as: León-Mancilla, B. H., et al. Physico-chemical characterization of collagen scaffolds for tissue engineering. *Journal of Applied Research and Technology* (2016), http://dx.doi.org/10.1016/j.jart.2016.01.001